

Thermodynamics and Phase Separation in Melt Blends of Polyethylene and Model Copolymers

Jangweon Rhee and Buckley Crist*

Department of Chemical Engineering, Northwestern University, Evanston, Illinois 60208

Received January 16, 1991; Revised Manuscript Received May 30, 1991

ABSTRACT: Binary blends of linear polyethylene (PE) and hydrogenated polybutadiene (HPB) are employed to evaluate the interaction parameter χ between chains containing different relative amounts of linear and ethyl-branched C_4H_8 repeat units. Conditions for liquid-liquid phase separation in the melt are determined unambiguously from the appearance of quench-crystallized blends which have been etched to define HPB-rich domains. For polyethylene and random poly(ethylene-co-butene-1) at 150 °C, $\chi = 0.022 Y_{br}^2$, where Y_{br} is the fraction of branched C_4H_8 repeat units. Domain sizes range from 0.1 to 16 μm , increasing with χ/χ_c and the time permitted for phase separation. Sizes observed for blends near the critical point compare favorably to those predicted by the linearized theory for spinodal decomposition.

Introduction

The recent discovery that olefin copolymers such as linear low-density polyethylene owe their interesting properties to the presence of chemically different chains¹ has spurred interest in the thermodynamics of systems containing random copolymers. Some studies have addressed phase separation of homopolymer A from random AB copolymers.²⁻⁷ In cases where the concentration of B repeats is small or where two AB copolymers of nearly the same composition are employed, miscible systems permit evaluation of the Flory-Huggins interaction parameter χ . This has been done by small-angle neutron scattering (SANS) for copolymers of styrene and acrylonitrile⁸ and ethylene and butene-1.⁹ It has been recognized that the isotopic substitution required for SANS experiments can influence the measurement of small interaction parameters.¹⁰ Only recently, however, was it found that isotope and chemical microstructure effects combine in a complicated manner¹¹ which may obscure the significance of χ measured by SANS.

Indeed, we have found such anomalous isotope effects in SANS studies of highly branched model copolymers of ethylene and butene-1; that is the subject of another report.¹² We present here the determination of χ by a variation of the cloud point method. Binary blends of linear polyethylene (PE) with a series of hydrogenated polybutadienes (HPB) are examined for phase separation in the melt state. HPB, formed by quantitative saturation of anionically polymerized polybutadiene, is a model for random ethylene-butene-1 copolymers which has the advantage of being nearly monodisperse.¹³ Because the linear and branched C_4H_8 repeat units are so similar, optical manifestation of phase separation is unreliable. The morphology of phase-separated melts is examined by scanning electron microscopy of quench-crystallized films. Beyond providing unequivocal evidence for the phase behavior of the molten blends, microscopy provides information on the phase separation process.

PE and HPB are here treated as copolymers of linear and ethyl-branched C_4H_8 units; HPB has a fraction Y_{br} of repeats which are branched, while PE has only linear units ($Y_{br} = 0$). For this homopolymer/random copolymer system we can write¹⁴

$$\chi = CY_{br}^2 \quad (1)$$

Ambiguity regarding the phase separation mechanism is avoided in systems having the critical composition ϕ_B^c .

The single-phase state is stable for $\chi < \chi_c$ and unstable for $\chi > \chi_c$, where χ_c and ϕ_B^c define the critical point:

$$\chi_c = (N_A^{-1/2} + N_B^{-1/2})^2/2 \quad (2)$$

$$\phi_B^c = N_A^{1/2}/(N_A^{1/2} + N_B^{1/2}) \quad (3)$$

Here, ϕ_B is the volume fraction and N_B is the degree of polymerization of HPB; the subscript A is for PE homopolymer. In these experiments χ is varied primarily through control of the branch concentration Y_{br} of the HPB component (eq 1). By determining the PE/HPB blend for which phase separation just occurs, eq 1 and 2 are combined to determine C . The constant C represents the interaction parameter between PE and atactic polybutene-1, i.e., HPB with $Y_{br} = 1$. This of course is a mean-field result, but no assumption regarding the dependence of χ on blend composition ϕ_B is involved; the interaction parameter is evaluated only at the critical volume fraction ϕ_B^c . The time dependence of phase separation in the unstable region ($\chi > \chi_c$) and reversibility were monitored to ensure that results are not subject to kinetic restrictions. The two-phase morphologies are interesting in their own right.

Experimental Section

Polymers and Blends. Unbranched polyethylenes were fractionated reference materials from NIST (SRM 1483 and SRM 1484); molecular weight and polydispersity were obtained from the supplier. The low and high molecular weight fractions are designated PE1 and PE2, respectively, in Table I. HPB's having various ethyl branch concentrations were prepared from anionically polymerized polybutadiene precursors by established methods.^{13,15} Characterization for molecular weight and fraction of 1,2 additions (equal to Y_{br}) was done on the polybutadienes by dilute-solution viscometry,^{16,17} and IR spectrophotometry,¹⁸ respectively. Polymers and chemical parameters are summarized in Table I, where the suffix on HPB_{xx} indicates Y_{br} (multiplied by 100). The polydispersity index of all HPB's is <1.1 for anionic products such as these; this was confirmed by GPC on polymers prepared similarly to those used here.^{13,18,19} Another important characteristic is that each HPB is largely or entirely amorphous at room temperature, while PE is about 70% crystalline. This difference is used to observe domains formed by phase separation in the melt.

Since the degree of polymerization N_A is nearly the same for the HPB's (average $N_B = 2100$), binary blends with PE1 ($N_A = 570$) have the critical composition at HPB volume fraction $\phi_B^c = 0.34$. Blends with $\phi_B = 0.35$ were prepared in dilute xylene solution at 140 °C, precipitated in cold methanol, filtered, and

Table I
Characterization of Polymers

sample	Y_{br}	N_w	N_w/N_n
PE1	0.00	570	1.11
PE2	0.00	2140	1.19
HPB22	0.22	2000	<1.1
HPB29	0.29	2310	<1.1
HPB31	0.31	2220	<1.1
HPB34	0.34	1980	<1.1
HPB38	0.38	1850	<1.1
HPB60	0.60	2130	<1.1

dried. Blends with $\phi_B = 0.50$ were similarly prepared for the nearly symmetric system ($N_A \approx N_B$) based on PE2.

Phase Separation and Morphology. Solution-blended powder in a small compression mold was placed in a 150 °C preheated press, held in the melt state for time $t = 20$ or 600 s and then removed and quenched in ice water. The times above are corrected for ca. 10 s required to melt the polymer. Chains are thus allowed to approach equilibrium from the initial state for time t , after which crystallization arrests any phase separation which occurred in the melt and preserves it for observation.^{3,4}

Quench-crystallized films (thickness from 0.4 to 1.0 mm) were microtomed at -100 °C to expose features away from the molded surfaces. Less crystalline HPB-rich regions were preferentially etched for 2 h at room temperature with a permanganic acid solution.²⁰ After suitable washing, the etched surface was sputter coated with Au and examined in a Hitachi S570 scanning electron microscope.

Results

Representative SEM images of quenched and etched samples are shown in Figures 1–3. Conventional banded spherulites of PE1 are shown in Figure 1a for reference; the unblended HPB components are noncrystalline and have no features visible by microscopy. The blend PE1/HPB29 contains the least branched model copolymer and hence has the smallest χ by eq 1. This system is one-phase in the melt, as indicated by the spherulitic texture in Figure 1b. These unbanded spherulites appear somewhat "open" because of dilution by 35% of noncrystallizable HPB29. The same blend, melted for only 20 s before quenching, is identical in appearance with Figure 1b (600 s in melt); there are no time effects.

Segregation of components in the melt is indicated by the morphology of the PE/HPB31 blend in Figure 2. There is no evidence of spherulites, and the size scale of the bi-continuous microstructure increases with time in the melt (Figure 2b versus Figure 2a). Hence the increase of Y_{br} from 0.29 to 0.31, corresponding to a 14% increment in χ by eq 1, suffices to cause the blend to be unstable. Further enhancing χ , by increasing Y_{br} as in the PE1/HPB60 system, results in larger features at short time (Figure 3a). After 600 s in the melt, coarsening has converted the bi-continuous morphology to discrete spheres of the minority component (Figure 3b).

Results of this part of the study are summarized in Table II, where it is seen that χ for the PE1/HPB system achieves the critical value of $\chi_c \approx 2.0 \times 10^{-3}$ when the copolymer has a branch fraction $0.29 < Y_{br} < 0.31$. This implies that the proportionality constant C in eq 1 is $C = 0.022 \pm 0.001$ at 150 °C (423 K). A further check on the accuracy of this value can be achieved through temperature changes. The PE1/HPB31 blend, having already been phase separated by melt aging for 20 s at 150 °C (Figure 2b), was reheated to 200 °C for 600 s, then quenched, and examined again. This previously phase-separated blend became one-phase in the melt at 200 °C as indicated by the "open" spherulites in Figure 4a (similar to Figure 1b). The rehomogenized blend was melted a third time at 150 °C for 20 s, during which the two-phase morphology appears once

more (Figure 4b). Such complete reversibility shows that thermodynamically controlled phase behavior is established without restrictions by kinetic effects. Furthermore, the 50 °K increase from 423 to 473 K decreases χ by 11%, assuming that $\chi \propto T^{-1}$, whereas χ_c is unchanged. This permits us to bracket C between 0.0207 and 0.0233, which is entirely consistent with the evaluation from changing Y_{br} . A more precise definition of C is not feasible because the degree of polymerization N (and hence χ_c) is subject to absolute uncertainties of $\sim 5\%$.

Similar experiments were done with blends based on the high molecular weight PE2. Here χ_c is smaller (see Table II) and phase separation is expected at a smaller value of Y_{br} for the HPB component. Indeed, the PE2/HPB22 blend was two-phase at 150 °C and one-phase at 180 and 200 °C, leading to $C = 0.021 \pm 0.001$; this agreement with the result from the PE1/HPB31 blend shows that χ , as embodied in eq 1, is independent of molecular weight of the unbranched component and independent of volume fraction over the modest range from $\phi_B = 0.35$ to $\phi_B = 0.50$.

These observations of miscibility or immiscibility in binary blends with different copolymers bear some similarity to the "miscibility map" approach suggested by Shiomi et al.²¹ One feature of the present method is reliance on what may be termed "macroscopic" phase separation, i.e., liquid-liquid domains with dimensions of order 0.1 μm or greater. These sizes are, however, some 2 orders of magnitude smaller than those seen by optical microscopy of demixing liquids.^{3–5} Some attempts were made to assess optical turbidity in coarsened two-phase blends such as those in Figure 3. No obvious effects were observed in films as thick as 1 mm. While this does not preclude cloud point or other scattering measurements, scattering power is no doubt small because of the similar physical properties of the blend components.

Discussion

Interaction Parameter. The foregoing experiments are summarized by rewriting eq 1:

$$\chi = 0.022 Y_{br}^2 \quad (4)$$

Recall that this applies to PE/HPB blends at 150 °C and corresponds to interactions between linear and branched C_4H_8 repeat units. A recent SANS study of interactions between PE and various HPB's in the one-phase melt⁹ yielded $C = 0.014$, which is 30% smaller than the present finding. This difference is attributed to the difficulty of measuring small positive χ by excess neutron scattering, particularly when compounded by interference from the hydrogen-deuterium isotope effect.¹¹ There is no doubt that the present result is more correct. For example, the SANS evaluation predicts the PE1/HPB31 blend to be one-phase at 150 °C (calculated χ/χ_c would be 0.68), whereas Figure 2 shows clearly that liquid-liquid phase separation has occurred. We are aware of no other experimental determinations of χ in ethyl-branched or similar copolymer systems. The present results is in general accord with estimates based on solubility parameters or heat of solution of low molecular weight alkanes, which predict C in the range from 0.012 to 0.041.⁹

The phase diagram for PE1/HPB blends is presented in Figure 5. Here the spinodal and coexistence lines have been calculated for $N_A = 570$ (PE1), $N_B = 2100$ (HPB), and the interaction parameter $\chi = \chi_c = 2.03 \times 10^{-3}$ is assumed to be independent of volume fraction ϕ_B . Points for the blends have been located according to eq 4. Those for PE1/HPB31 through PE1/HPB60 correspond to

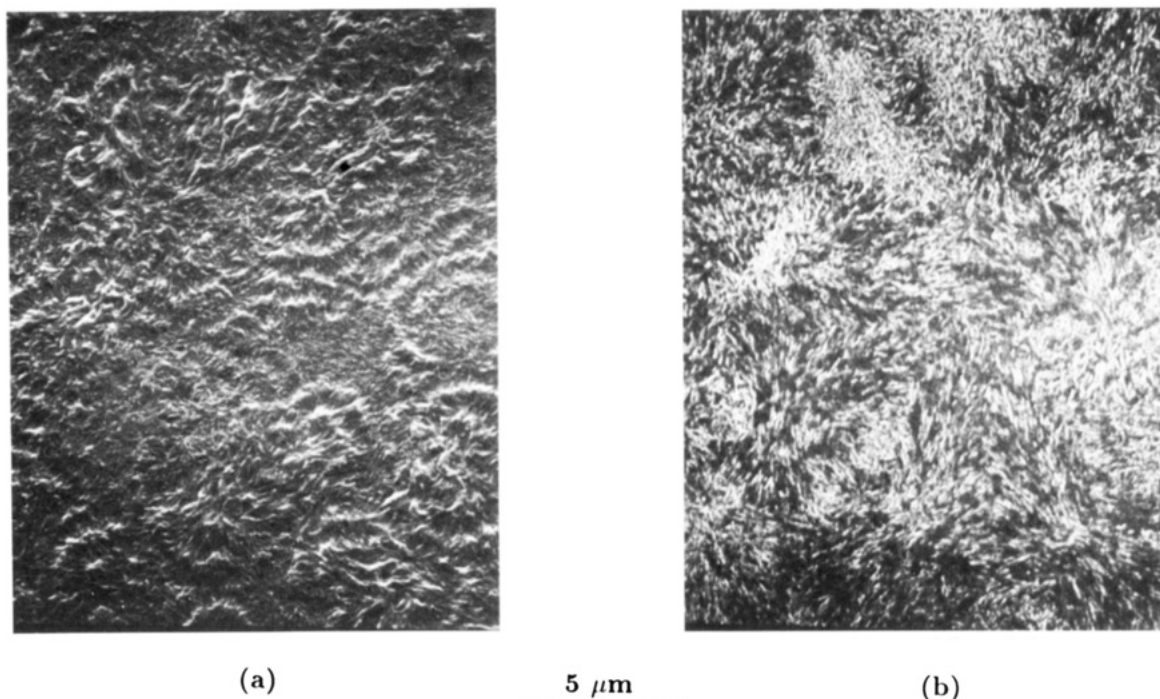


Figure 1. SEM image of spherulitic morphologies in quench-crystallized PE1 (a) and PE1/HPB29 (b). These are indicative of a one-phase melt.

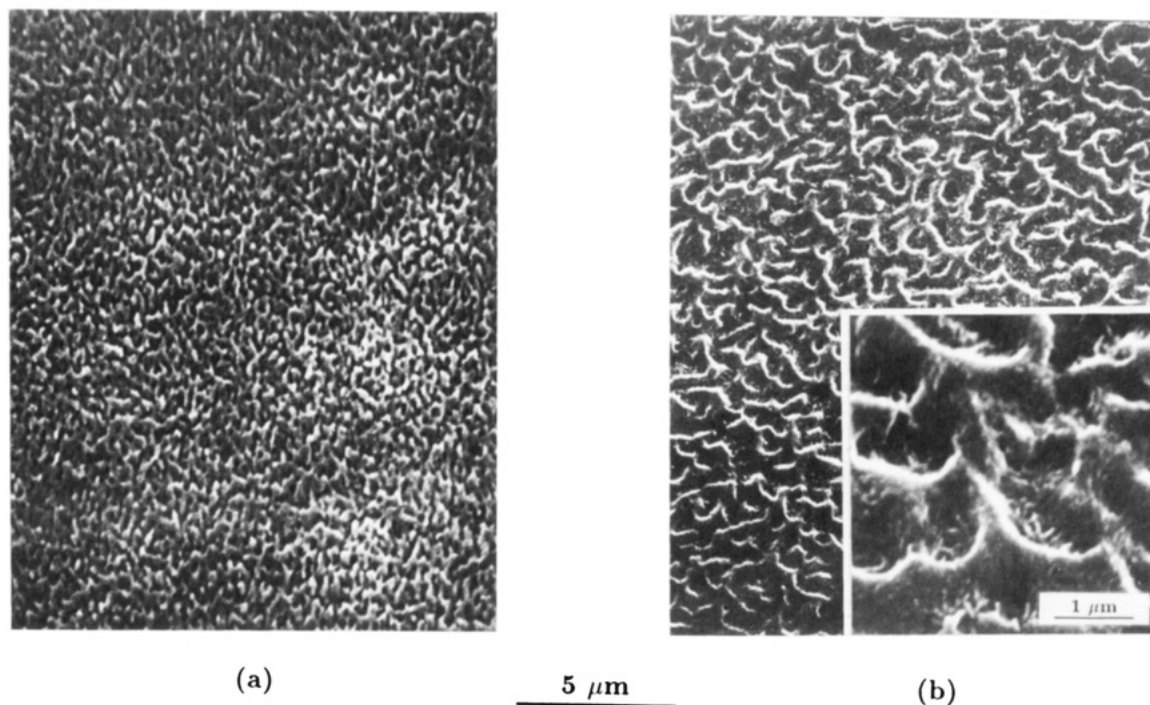


Figure 2. SEM image of PE1/HPB31 quench crystallized after melting for 20 (a) and 600 s (b). Preferential etching causes the HPB-rich areas to appear as darker regions rimmed in white on the bottom edge.

increasingly severe "quenches" into the unstable region of the phase diagram ($\chi > \chi_c$). The present approach is unusual in that temperature and molecular weight are held constant, and hence the intrinsic mobility factors (self-diffusion coefficients of the blend components) are nearly invariant. Conventional methods for increasing quench depth—decreasing temperature (for systems with an upper critical solution temperature) or increasing degree of polymerization N —decrease intrinsic mobilities.

Phase Separation Microstructures. Morphological characteristics of the two-phase blends are presented in Table III. Mean intercept length \bar{l} and volume fraction

of the HPB-rich regions f_B were evaluated by standard line segment analyses,²² employing higher magnification images were required. It should be pointed out that the etching/microscopy method used here is not suitable for evaluating amplitudes of concentration fluctuations. Therefore no value of f_B is reported for blends in which it is suspected that the concentration profile is nearly sinusoidal (short time and shallow quench, e.g., Figure 2a). The line segment analysis for \bar{l} still applies, however, for such systems which lack well-defined phase boundaries. Another point is that the measured value of f_B is increased somewhat by the larger thermal contraction of the PE-

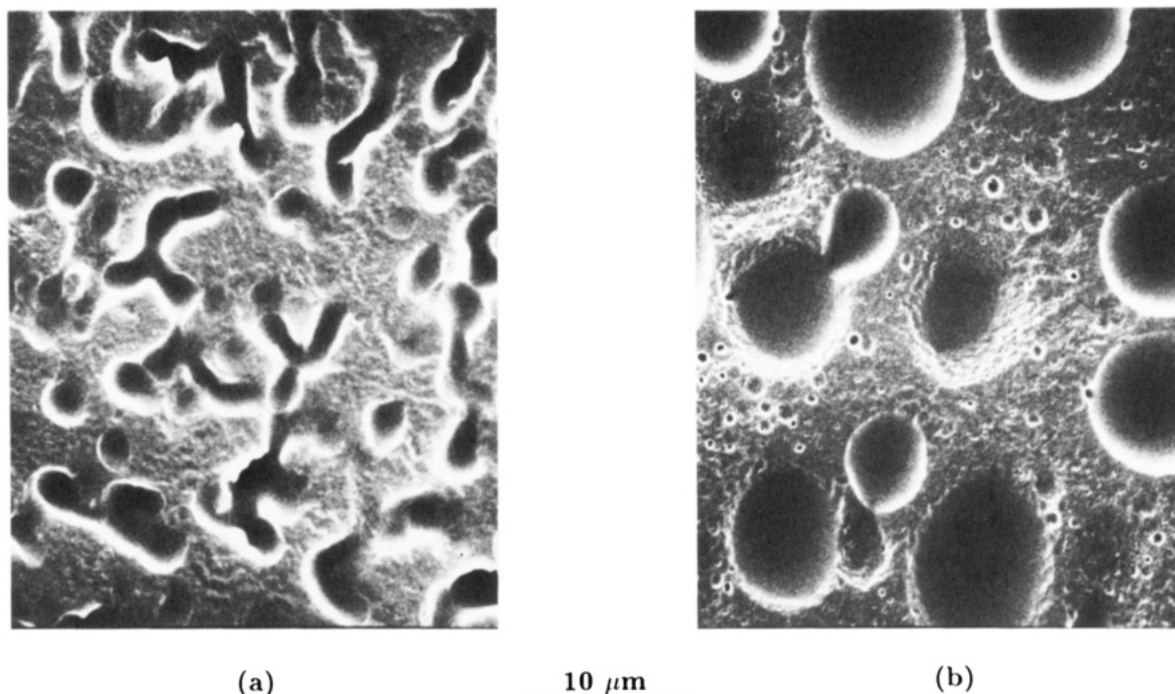


Figure 3. SEM image of PE1/HPB60 quench crystallized after melting for 20 (a) and 600 s (b). Note the change in magnification compared to that in Figures 1, 2, and 4.

Table II
Binary Blends

blend	φ_B	$10^3 \chi_c$	temp, °C	phase
PE1/HPB29	0.35	1.97	150	one
PE1/HPB31	0.35	1.99	150	two
			200	one
PE1/HPB34	0.35	2.07	150	two
PE1/HPB38	0.35	2.12	150	two
PE1/HPB60	0.35	2.02	150	two
PE2/HPB22	0.50	0.97	150	two
			180	two
			200	one
PE2/HPB60	0.50	0.94	150	two

rich phase on cooling to room temperature; this small effect is ignored. Equilibrium volume fractions f_B^{eq} were determined from the coexistence curve in Figure 5.

Since the phase-separated morphologies originated from spinodal decomposition, it is of interest to consider the kinetically favored wavelength λ_m . This is the characteristic size one expected at the first stage of demixing, where the linearized Cahn-Hilliard theory²³ for spinodal decomposition is most applicable. Calculations based on Binder's²⁴ analysis of phase separation in polymers are described in the Appendix and presented in Table III. It should be noted that the linearized Cahn-Hilliard wavelength λ_m decreases from $22\bar{R}_g$ to $3\bar{R}_g$ as the driving force χ/χ_c is increased from 1.06 to 8.4, the range of the current experiments. \bar{R}_g is a root mean square radius of gyration for the mixture of PE and HPB chains: see the Appendix. The growth rates R_m for microstructures having λ_m are also calculated and presented in the Appendix.

Consider first the characteristic length \bar{l} for the PE1/HPB system. This size scale for the phase-separated microstructure increases with time for each blend (as seen in Figures 2 and 3), and, for $t = 20$ s, \bar{l} increases with χ/χ_c . It should be noted, however, that \bar{l} is nearly equal to the spinodal wavelength λ_m for the "shallowest quench" case (PE1/HPB31, $\chi/\chi_c = 1.06$). Such equivalence between \bar{l} and λ_m is expected in the early stages of spinodal decomposition, for which the conventional signature is an exponential time dependence of the magnitude of the

concentration fluctuations as determined from scattered intensity.^{23,24} The etching/microscopy technique employed here does not permit measurement of concentration amplitudes, but we can calculate the linearized growth factor R_m a priori because the intrinsic diffusivities of the chains are known. This calculation is presented in the Appendix as the exponent $R_m t$ in the linearized growth expression for $t = 20$ s. For the shallow-quench PE1/HPB31 blend in question, $R_m t = 3.0$, which is moderate and consistent with early stages. Scattering experiments on demixing polymers generally indicate that the linearized theory is applicable for $R_m t \leq 1.1$.^{6,25-27} The range of exponents $R_m t$ for which this approximation is valid depends of course on the composition dependencies of the interdiffusion coefficient and the second derivative of free energy for the particular blend being considered.²³ Returning to the present experiment, $R_m t > 50$ for all other blends and times in the PE1/HPB system, so appreciable coarsening has occurred ($\bar{l} > \lambda_m$). It is interesting that $\bar{l} \approx 10 \mu\text{m}$ after 600 s for the three blends with $1.2 < \chi/\chi_c < 4$. This may be coincidental, but it may reflect an abrupt slowing of the coarsening rate at a characteristic size such as occurs in Ostwald ripening.

The high molecular weight blend PE2/HPB22 is also near the critical point at 150 °C ($\chi/\chi_c = 1.10$). Again we see that $\bar{l} \approx \lambda_m$ after 20 s, when agreement with linearized theory is expected since $R_m t = 1.2$ (see Table IV). A modest size increase due to nonlinear effects is evident after 600 s ($\bar{l} = 2\lambda_m$, $R_m t = 36$). This system was used to examine demixing even closer to the critical point. The phase-separated blend was homogenized by heating above 200 °C (600 s) and quenching. Its microstructure at this stage was "open" spherulites similar to that in Figure 4a. The blend was reheated for $t = 20$ s at $T = 180$ °C, at which $\chi/\chi_c = 1.03$, and then quenched for observation by SEM. Micrographs are shown in Figure 6 for the same blend demixed at 150 °C (Figure 6a) and at 180 °C (Figure 6b). Although the calculated wavelength λ_m has doubled to 0.50 μm , the observed size has decreased from 0.22 μm to $\bar{l} = 0.13 \mu\text{m}$. For this shallow quench with large- N chains

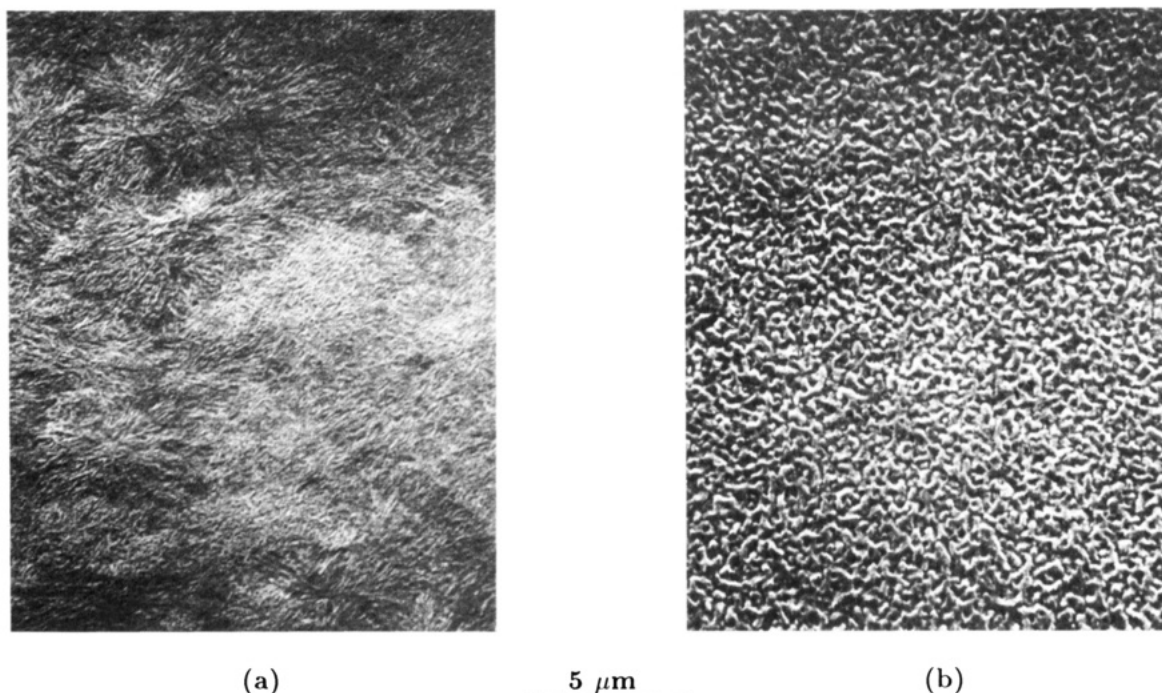


Figure 4. SEM image of the two-phase PE1/HPB31 sample of Figure 2a quench crystallized after remelting at 200 °C for 600 s (one phase: a) and after a third melting at 150 °C, 20 s (two phase: b).

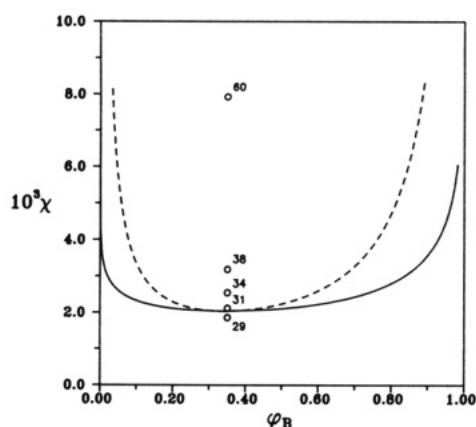


Figure 5. Calculated spinodal (---) and coexistence (—) lines for PE/HPB blends; $N_A = 570$, $N_B = 2100$, $\chi_c = 2.0 \times 10^{-3}$, $\phi_B^c = 0.34$. Points are for the PE1/HPB blends at 150 °C, labeled according to $100Y_{br}$.

Table III
Characteristics of Two-Phase Melts at 150 °C

blend	χ/χ_c	time, s	\bar{l} , μm	λ_m , μm	f_B	f_B^{eq}
PE1/HPB31	1.06	20	0.3 ₄	0.22		0.49
		600	0.9 ₀		0.51	
PE2/HPB22	1.10	20	0.2 ₂	0.26		0.50
		600	0.5 ₃		0.54	
PE1/HPB34	1.23	20	1.3	0.11	0.43	0.45
		600	10.5		0.39	
PE1/HPB38	1.50	20	1.7	0.08	0.38	0.41
		600	10.8		0.39	
PE1/HPB60	3.92	20	6.3	0.03	0.31	0.37
		600	10.0		0.38	
PE2/HPB60	8.43	20	1.5	0.05	0.52	0.50
		600	16.2		0.55	

the growth exponent $R_m t = 0.12$; the system has been arrested in the very early stage of spinodal decomposition. One expects that thermally driven concentration fluctuations, which favor the relatively rapid growth of features with dimensions less than λ_m ,²⁸ may be operative. Strobl's analysis²⁹ of a symmetric polymer system at $\chi/\chi_c = 1.025$ shows that initial fluctuations have $\bar{l} \approx 0.3\lambda_m$, which is the

same ratio as observed in Figure 6b. While such agreement is satisfying, one must realize that growth by this fluctuation mechanism depends on the previous state of the sample; such information is lacking in the PE2/HPB22 blend, which was quench crystallized before the demixing process. Nevertheless, this is the first direct space observation of small features arising from fluctuations. Okada and Han have analyzed scattering measurements very near the critical solution temperature for fluctuation microstructure in a polystyrene/poly(vinyl methyl ether) blend.³⁰

The experimental volume fractions of HPB-rich regions, f_B , are seen to decrease moderately, from about 0.5 to 0.4, in the series from PE1/HPB31 to PE1/HPB60. This trend and the absolute values are followed nicely by f_B^{eq} values from the phase diagram. No such drift of f_B with χ is expected for the symmetric PE2/HPB system. A more subtle connection between the phase diagram and observed morphology is indicated by the very fine lamellar structure seen within the HPB-rich regions for PE1/HPB31, 600 s (inset in Figure 2b). The coexistence curve shows that the equilibrium composition for the HPB-rich phase contains 50% PE1. When quenched, this relatively large amount of crystallizable polyethylene in the HPB-rich domains forms lamellar bundles which are subsequently exposed during etching. It is possible that these features are portions of larger spherulites which grow through both PE-rich and HPB-rich domains, similar to the morphology of polypropylene/poly(propylene-co-ethylene) blends reported by Inaba et al.⁴ We think it unlikely that these lamellae result from ordering of the evolving domains in the late stages of spinodal decomposition.^{31,32} Those effects result from short-range correlations of the concentration profiles over multiples of the size scale \bar{l} , while the features in the inset of Figure 2b are clearly of a size less than $\bar{l} = 0.9 \mu\text{m}$. A final point on morphology involves the "deep-quench" blends having the largest χ/χ_c . The bicontinuous microstructure of the asymmetric PE1/HPB60 blend is seen to coarsen with the evolution of spherical domains of the minority HPB component (Figure 3b). The symmetric PE2/HPB60 blend, on the other

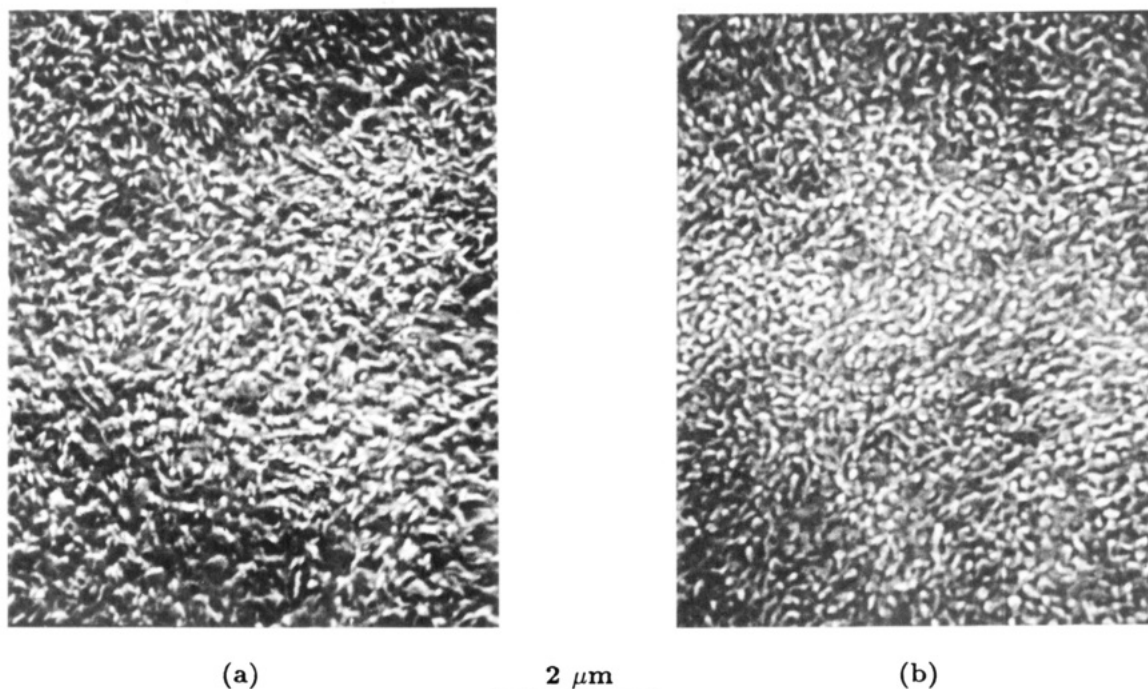


Figure 6. SEM image of PE2/HPB22 after spinodal decomposition for 20 s at 150 °C, $\chi/\chi_c = 1.10$ (a), and at 180 °C, $\chi/\chi_c = 1.03$ (b).

hand, maintains the bicontinuous microstructure when coarsening to $\bar{l} = 16 \mu\text{m}$ after 600 s (no figure is shown). This is expected, as no decrease in surface energy can be achieved by transforming to discrete particles of either phase in this $f_B = 0.5$ system.

Conclusions

The morphology of quench-crystallized blends of polyethylene and model ethylene-butene-1 copolymers is shown to indicate the presence or absence of liquid-liquid phase separation in the melt. For systems with critical composition, the interaction parameter for unbranched polyethylene and poly(butene-1) is $\chi = 0.022$ for C_4H_8 repeat units at 150 °C (reference volume of $71.6 \text{ cm}^3/\text{mol}$). This quantity indicates that copolymers having more than 60 ethyl branches per 1000 backbone carbon atoms ($Y_{br} > 0.21$) are required for phase separation from unbranched polyethylene in systems with molecular weight $M = 118\,000$ ($N = 2100$). More work is required to establish the relation between this result, derived from binary blends, and phase separation observed in multicomponent systems such as linear low-density polyethylene.¹

PE/HPB blends, in which crystallization of PE arrests demixing in the liquid state, provide convenient systems for examining phase separation either near the critical point or deep in the two-phase diagram. The etching/microscopy method employed here uses crystallinity as the "contrast factor" for indirect observation of liquid-state morphology. The formation and destruction of concentration differences over distances of $\sim 0.1 \mu\text{m}$ are seen to occur reversibly, without kinetic restrictions for the 20-s time resolution of this method, for systems within 5% of the critical point. Domain sizes near the critical point are nearly the same as those predicted by the linearized theory for spinodal decomposition, provided demixing is observed at suitably short times ($R_m t$ of order 1). We are able to calculate the growth rate R_m from first principles, since the diffusion coefficients of the blend components are known.

Morphology of coarsened microstructures is in accord with qualitative expectations for both symmetric and

asymmetric systems. The microscopy technique employed here has spatial resolution better than $0.05 \mu\text{m}$, permitting direct observation of the early stage of spinodal decomposition for shallow quenches. It also gives reliable volume fractions for equilibrium domains developed in the melt.

Acknowledgment. This research was supported by the Gas Research Institute, Physical Sciences Division (Contract No. 5084-260-1051). We are indebted to H. Swei for developing the etching and microscopy technique and to Profs. M. Olvera de la Cruz and P. Voorhees for many helpful discussions.

Appendix

Evaluation of λ_m . The linearized theory for spinodal decomposition is applicable to the first stages of the phase separation process. The kinetically favored length scale for demixing, λ_m , is expressed in terms of the wavevector q_m :

$$\lambda_m = 2\pi/q_m \quad (\text{A-1})$$

We employ the following expressions, which are based on the treatment of Binder²⁴ as reviewed by Hashimoto:³³

$$q_m^2 = \frac{3}{2R_g^2} \left(1 - \frac{\chi_s}{\chi}\right) \quad \left(1 - \frac{\chi_s}{\chi} \ll 1\right) \quad (\text{A-2})$$

$$q_m^2 = \frac{1}{R_g^2} \left(\frac{2\chi}{\chi_s}\right)^{1/2} \quad \left(\frac{\chi}{\chi_s} \gg 1\right) \quad (\text{A-3})$$

Equation A-2 is appropriate for shallow quenches and eq A-3 for deep quenches. Here, χ_s is the value of χ on the spinodal line:

$$\chi_s = \frac{1}{2} \left[\frac{1}{\varphi_A N_A} + \frac{1}{\varphi_B N_B} \right] \quad (\text{A-4})$$

The quantity $\overline{R_g^2}$ is a mean square radius of gyration for

Table IV
Maximum Spinodal Growth Rates at 150 °C

blend	χ/χ_c	D_{app} , 10^{-12} cm ² /s	q_m , μm^{-1}	$R_m \times 20$, s
PE2/HPB22	1.10	2.1	24.2	1.2
PE1/HPB31	1.06	3.6	28.6	3.0
PE1/HPB34	1.23	16	57.1	51
PE1/HPB38	1.50	37	78.5	228

the combination of A and B Gaussian chains:

$$\bar{R}_g^2 = \frac{N_A N_B (\varphi_B a_A^2 + \varphi_A a_B^2)}{6(\varphi_A N_A + \varphi_B N_B)} \quad (\text{A-5})$$

Degree of polymerization N_i and volume fraction φ_i have been introduced in the text; a_i is the effective length of a repeat unit so that $\bar{R}_{gi}^2 = N_i a_i^2 / 6$ for each component.

Equation A-2 (shallow quench) was used for all blends except the two containing HPB60; eq A-3 (deep quench) was used for those. Since all systems had the critical composition, χ_s is equal to χ_c (eq 2 in the text). Values of a_i were obtained from measurements of coil dimensions at 150 °C for PE and HPB.^{12,34} \bar{R}_g is 90 ± 2 Å for all blends in the PE1/HPB system and 151 ± 3 Å for the PE2/HPB blends. The calculated spinodal wavelengths λ_m appear in Table III.

Evaluation of the Growth Rate $R(q)$. Let $S_q(t)$ be the Fourier component of the composition fluctuation in direct space. Again restricting ourselves to the linearized theory of spinodal decomposition, this quantity grows exponentially with time:

$$S_q(t) = S_q(0)e^{R(q)t} \quad (\text{A-6})$$

This relation is expected to hold for modest values of the exponent, i.e., for $R(q)t \leq 1$. The growth rate $R(q)$ depends on wavevector q according to^{24,33}

$$R(q) = q^2 D_{app} \left(1 - \frac{q^2}{2q_m^2} \right) \quad (\text{A-7})$$

It is largest for $q = q_m$:

$$R_m = q_m^2 D_{app} / 2 \quad (\text{A-8})$$

Here, q_m is defined by eq A-2 for shallow quenches.

The mutual diffusion coefficient of A and B chains, including thermodynamic slowing down for systems near the spinodal line, is given by

$$D_{app} = \frac{D_A D_B (\varphi_A N_A + \varphi_B N_B)}{\varphi_A N_A D_A + \varphi_B N_B D_B} \left(\frac{\chi - \chi_s}{\chi_s} \right) \quad (\text{A-9})$$

Here, D_i is the self-diffusion coefficient of the polymer chain. Reptation is appropriate for highly entangled chains:

$$D_i = k_i N_i^{-2} \quad (\text{A-10})$$

Diffusion coefficients at 150 °C were determined from previous studies on PE³⁵ and HPB.³⁶ It is assumed that k for a $Y_{br} = 0.08$ polymer is applicable to HPB with higher concentrations of ethyl branches. D_{app} and $R_m \times 20$ s were calculated for the blends indicated in Table IV. On increasing the quench depth in the PE1/HPB system, R_m increases by nearly 2 orders of magnitude. R_m is smallest in the PE2/HPB22 blend because of larger N (smaller D_i).

It is noted that the mutual diffusion coefficient D_{app} in eq A-9 corresponds to the "slow-mode" formulation. This stems from the assumption of incompressibility of the polymer fluid.²⁴ Experimental studies of mutual diffusion indicate that the "fast-mode" expression is more correct.³⁷ This distinction is moot in the present study because, quite accidentally, slow- and fast-mode calculations of D_{app} are within 20% of one another for the PE1/HPB system. The two theories give nearly identical values of D_{app} for the symmetric PE2/HPB system, as expected.

References and Notes

- (1) Mirabella, F. M.; Westphal, S. P.; Fernando, P. L.; Ford, E. L.; Williams, J. G. *J. Polym. Sci., Part B: Polym. Phys.* **1988**, *26*, 1995.
- (2) Lohse, D. J. *Polym. Eng. Sci.* **1986**, *26*, 1500.
- (3) Inaba, N.; Sato, K.; Suzuki, S.; Hashimoto, T. *Macromolecules* **1986**, *19*, 1690.
- (4) Inaba, N.; Yamada, T.; Suzuki, S.; Hashimoto, T. *Macromolecules* **1988**, *21*, 407.
- (5) Strobl, G. R.; Bendler, J. T.; Kambour, R. P.; Shultz, A. R. *Macromolecules* **1986**, *19*, 2683.
- (6) Takenaka, M.; Izumitani, T.; Hashimoto, T. *Macromolecules* **1987**, *20*, 2257.
- (7) Izumitani, T.; Takenaka, M.; Hashimoto, T. *J. Chem. Phys.* **1990**, *92*, 3213.
- (8) Schmitt, B. J.; Kirste, R. G.; Jelenic, J. *Makromol. Chem.* **1980**, *181*, 1655.
- (9) Nicholson, J. M.; Finerman, T. M.; Crist, B. *Polymer* **1990**, *31*, 2287.
- (10) Wignall, C. D.; Bates, F. S. *Makromol. Chem., Macromol. Symp.* **1988**, *15*, 105.
- (11) Sakurai, S.; Hasegawa, H.; Hashimoto, T.; Hargis, I. G.; Aggarwal, S. L.; Han, C. *Macromolecules* **1990**, *23*, 451.
- (12) Rhee, J.; Crist, B., submitted to *J. Chem. Phys.*
- (13) Krigas, T. M.; Carella, J. M.; Struglinski, M. J.; Crist, B.; Graessley, W. W.; Schilling, F. C. *J. Polym. Sci., Part B: Polym. Phys.* **1985**, *23*, 509.
- (14) Paul, D. R.; Barlow, J. W. *Polymer* **1984**, *25*, 487.
- (15) Rachapudy, H.; Smith, G. G.; Raju, V. R.; Graessley, W. W. *J. Polym. Sci., Part B: Polym. Phys.* **1979**, *17*, 1211.
- (16) Colby, R. H.; Fetters, L. J.; Graessley, W. W. *Macromolecules* **1987**, *20*, 2226.
- (17) Mays, J.; Hadjichristidis, N.; Fetters, L. J. *Macromolecules* **1984**, *17*, 2723.
- (18) Carella, J. M. Ph.D. Thesis, Northwestern University, 1981.
- (19) Wild, L. Quantum Chemicals, private communication.
- (20) Bassett, D. C.; Hodge, A. M. *Proc. R. Soc. London, Ser. A* **1981**, *377*, 25.
- (21) Shiomi, J.; Karasz, F. E.; MacKnight, W. J. *Macromolecules* **1986**, *19*, 2274.
- (22) Underwood, E. E. *Quantitative Stereology*; Addison-Wesley Co.: Menlo Park, CA, 1970; p 81ff.
- (23) Hilliard, J. E. In *Phase Transformations*; Aaronson, H. I., Ed.; American Society for Metals: Metals Park, OH, 1970; Chapter 12.
- (24) Binder, K. *J. Chem. Phys.* **1983**, *79*, 6387.
- (25) Izumitani, T.; Hashimoto, T. *J. Chem. Phys.* **1985**, *83*, 3694.
- (26) Hashimoto, T.; Itakura, M.; Shimidzu, N. *J. Chem. Phys.* **1985**, *85*, 6773.
- (27) Bates, F. S.; Wiltzius, P. *J. Chem. Phys.* **1989**, *91*, 3258.
- (28) Cook, H. E. *Acta Metall.* **1970**, *18*, 297.
- (29) Strobl, G. R. *Macromolecules* **1985**, *18*, 558.
- (30) Okada, M.; Han, C. C. *J. Chem. Phys.* **1986**, *85*, 5317.
- (31) Takenaka, M.; Izumitani, T.; Hashimoto, T. *J. Chem. Phys.* **1990**, *92*, 4566.
- (32) Hashimoto, T.; Takenaka, M.; Jinnai, H. *J. Appl. Crystallogr.*, in press.
- (33) Hashimoto, T. *Phase Transformations* **1988**, *12*, 47.
- (34) Arnett, R. L.; Stacy, C. J. *J. Phys. Chem.* **1973**, *77*, 1986.
- (35) Klein, J.; Briscoe, B. J. *Proc. R. Soc. London, Ser. A* **1979**, *365*, 53.
- (36) Bartels, C.; Crist, B.; Graessley, W. W. *Macromolecules* **1984**, *17*, 2702.
- (37) Composto, R. J.; Kramer, E. J.; White, D. M. *Nature* **1987**, *328*, 234.